CHINESE OPTICS LETTERS

Vol. 19, No. 4 | April 2021

Optical beam splitting and asymmetric transmission in bi-layer metagratings

Qiangshi Shi (施强石)[1,2], Xia Jin (金 霞)[1], Yangyang Fu (伏洋洋)[3], Qiannan Wu (吴倩楠)[4], Cheng Huang (黄 程)[1], Baoyin Sun (孙宝印)[2*], Lei Gao (高 雷)[2], and Yadong Xu (徐亚东)[2**]

[1] College of Energy, Soochow University, Suzhou 215006, China

[2] School of Physical Science and Technology, Soochow University, Suzhou 215006, China

[3] College of Science, Nanjing University of Aeronautics and Astronautics, Nanjing 211106, China

[4] School of Science, North University of China, Taiyuan 030051, China

*Corresponding author: bysun@suda.edu.cn

**Corresponding author: ydxu@suda.edu.cn

Received August 26, 2020 | Accepted October 19, 2020 | Posted Online February 2, 2021

In this work, inspired by advances in twisted two-dimensional materials, we design and study a new type of optical bi-layer metasurface system, which is based on subwavelength metal slit arrays with phase-gradient modulation, referred to as metagratings (MGs). It is shown that due to the found reversed diffraction law, the interlayer interaction that can be simply adjusted by the gap size can produce a transition from optical beam splitting to high-efficiency asymmetric transmission of incident light from two opposite directions. Our results provide new physics and some advantages for designing subwavelength optical devices to realize efficient wavefront manipulation and one-way propagation.

Keywords: asymmetric transmission; high efficiency; bi-layer metagratings; abrupt phase control.

DOI: 10.3788/COL202119.042602

1. Introduction

Optical phase-gradient metasurfaces (PGMs)[1–4] have attracted much attention in the past few years due to their fundamental interest and practical importance. Typically, PGMs are constructed as periodic gratings consisting of a supercell spatially repeated along an interface, and each supercell consists of m unit cells (i.e., meta-atoms), with m being an integer. The key idea of PGMs is to introduce an abrupt phase shift covering the range of 0 to 2π discretely through m unit cells of different optical responses to ensure complete control of the outgoing wavefront. The phase gradient provides a new degree of freedom for the manipulation of light propagation, allowing a number of intriguing optical phenomena or metadevices[5–17], such as the generalized Snell's law (GSL)[5], metalenses[6], the photonic spin Hall effect[8], wavefront controlling[10,13], and perfect anomalous diffraction[14–16].

Inspired by the concept of PGMs, recently, subwavelength metal slit arrays with phase-gradient modulation, referred as metagratings (MGs)[18–25], have been used to effectively manipulate wavefronts and realize new phenomena or effects beyond those predicted by the GSL. It is found that anomalous transmission and reflection through higher-order diffraction can be completely reversed by changing the integer parity of the MG design, and it obeys a new set of m-dependent diffraction equations[21].

Alternatively, angularly asymmetric diffraction was observed theoretically and experimentally in MGs[22,23], stemming from the loss-induced suppression of higher-order diffraction[24].

Although great progress has been made with regard to single-layer MGs, the study of the multilayer system composed of the single-layer MG is still relatively rare. In recent years, in condensed matter physics, the interaction between layers of two-dimensional (2D) materials[26], such as graphene and MoS_2, has led to many unusual physical properties, such as topologic transition[27]. Similarly, in the multilayer system composed of the single-layer MG, it is highly desired to explore whether the interlayer interactions will also bring some new phenomena that cannot be observed in a single-layer system. Although many efforts have been devoted to the study of few-layer metasurfaces[28], distinctive effect and applications triggered by the new set of diffraction laws in MG systems require further exploration.

2. Models and Theories

In this work, as a concrete example, we design and study a bi-layer MG with a relatively simple structure operating at the visible frequencies, and each layer of MG contains only two units ($m = 2$). We will show that the interlayer interaction controlled by simply adjusting the interlayer gap size can produce a transition from efficient optical beam splitting to high-contrast asymmetric transmission of light incident from two opposite directions. In particular, for positive normal incidence (PI), the transmission is about 2%, while for negative normal incidence (NI), the transmission is about 92.5%. Although the metal, which is often considered to be with high loss at visible wavelengths, is involved in the designed MG system, the efficiency of optical beam splitting is much higher than that in previously reported dielectric PGMs[29].

Before exploring the bi-layer MGs, we first consider two single-layer MGs (i.e., MG-1 and MG-2, see Figs. 1(a) and 2(a), respectively) used to form the bi-layer system and illustrate their diffraction characteristics. The working wavelength of interest is $\lambda = 650$ nm. Figure 1(a) displays schematically the geometry of MG-1, a periodic metallic slit array (gray region) filled with two different kinds of media (colored blue regions) alternatively, forming a supercell containing two unit cells (i.e., $m = 2$). The period length of the supercell is $p_1 = 2a = \sqrt{2}\lambda/2$, $w = 180$ nm, and the thickness is $h = 0.5\lambda$. Note that the asymmetric transmission performance of the bi-layer MG we designed is largely affected by the groove width, which physically determines the coupling effect between the adjacent metal slits. After numerical calculations, it is found that $w = 180$ nm is a good candidate. The metal is silver with $\varepsilon_m = -17.86 + 0.715i$[30], and two filled media are air with $\varepsilon = \mu = 1$ and an impedance-matched material with $\varepsilon = \mu = 2$, respectively. Later, we will show that all results in this ideal case can still be seen in the impedance-mismatched case.

When a TM polarized light is incident from up down onto the designed MG-1, it achieved an abrupt phase shift of π between two adjacent slits at the transmitted interface, leading to a phase gradient or effective momentum, i.e., $\xi_1 = \Delta\varphi/\Delta x = \sqrt{2}k_0$, where $k_0 = 2\pi/\lambda$ is the wave vector in air. After being scattered by the MG, the diffractions of transmitted and reflected light are governed by the following[21]:

$$k_x^{r,t} = k_x^{\text{in}} \pm nG_1, \tag{1}$$

where $G_1 = \xi_1 = 2\pi/p_1 = \sqrt{2}k_0$ is the reciprocal lattice vector, and the integer n is the diffraction order. Due to $G_1 > k_0$, for normal incidence, such MG-1 only survives $n = 0$ order in both transmission and reflection, because other diffracted waves are evanescent waves that do not contribute to the far fields [see the iso-frequency diagram shown by Fig. 1(b)]. Further, based on the concept of parity reversal[21], the condition $L = m + n$ (L is the number of times that the light passes through the slits) shows that the diffraction order of $n = 0$ takes a round-trip process (i.e., $L = 2$), due to $m = 2$, which means that the incident wave is completely reflected. The critical angle of $n = 0$ is $\theta_c = \arcsin(\xi/k_0 \pm 1) \cong \pm 24.5°$. For $\theta_{\text{in}} \geq 24.5°$ and $\theta_{\text{in}} \leq -24.5°$, as shown by the red arrows in Fig. 1(b), the diffraction order of $n = 0$ is closed, and then the incident light will be diffracted into the order of $n = \pm 1$. In this way, it is $L = m + n = 1$, which means that the diffracted light enters the transmission channel, and the direction of diffracted light is completely reversed from the reflection side to the transmission side. These discussed physics has been solidly confirmed by numerical simulations carried out using COMSOL Multiphysics. Figures 1(c) and 1(d) illustrate the obtained numerical results of field patterns for incident Gaussian beams with $\theta_{\text{in}} = 0°$ and 45° onto MG-1, respectively. One can clearly see that MG-1 reflects almost all of the normally incident light back [Fig. 1(c)]. For $\theta_{\text{in}} = 45°$ [Fig. 1(d)], most of incident light transmits through MG-1, with the refraction angle that is indeed $\theta_t = -45°$.

Alternatively, Fig. 2(a) displays schematically the geometry of MG-2 designed based on the binary unit structure of MG-1. Its supercell can still be considered to contain two unit cells (i.e., $m = 2$), and its period length is $p_2 = 2p_1$. Likewise, when a TM light is incident from up down onto the designed MG-2, the abrupt phase shift between two adjacent slits at the transmitted interface is still π, and the phase gradient is $\xi_2 = \Delta\varphi/\Delta x = \sqrt{2}k_0$. In this case, the diffractions of both transmitted and reflected light obey the following:

$$k_x^{r,t} = k_x^{\text{in}} \pm nG_2, \tag{2}$$

where $G_2 = \xi_2 = 2\pi/p_2 = \sqrt{2}k_0$. In MG-2, the diffraction orders of $n = 0$ and $n = \pm 1$ are all open for $k_x^{\text{in}} = 0$ [see Fig. 2(b)]. However, the condition $L = m + n$ tells us that the diffraction orders of $n = \pm 1$, which directly take one-pass propagation, are preferential to $n = 0$ order with the round-trip process. Therefore, the diffraction light will take the transmission channel, and it is split equally into two beams with outgoing angle $\theta_t = \pm 45°$. Figure 2(c) shows the numerical simulations obtained using COMSOL Multiphysics, where MG-2 splits the Gaussian

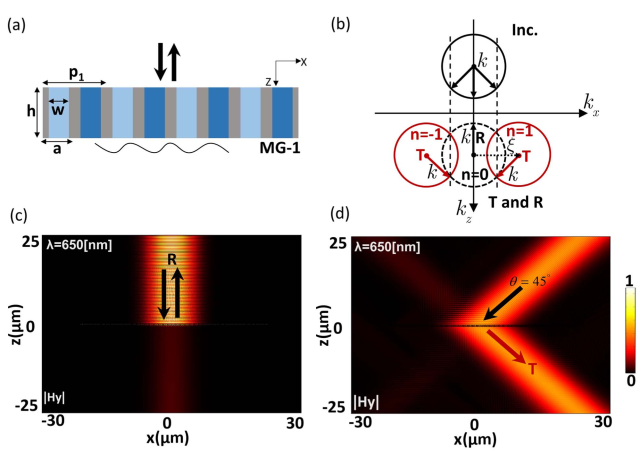

Fig. 1. (a) Structure of designed MG-1, a periodic metallic slit array (gray region) filled with two different kinds of media (colored blue regions) alternatively, forming a supercell containing two unit cells (i.e., $m = 2$). (b) Iso-frequency diagram indicating all possible diffraction orders. (c) and (d) are the magnetic field patterns for incident light with two different incident angles. The working wavelength is $\lambda = 650$ nm.

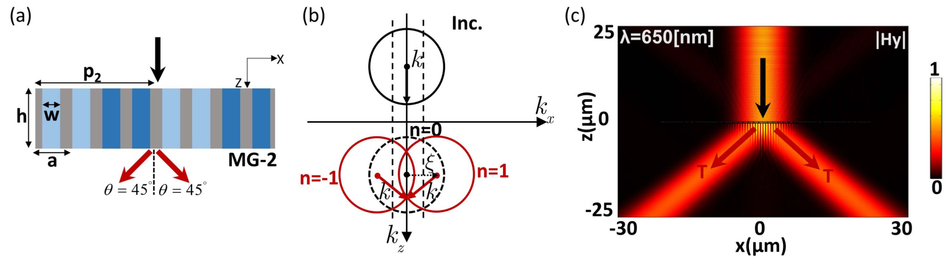

Fig. 2. (a) Structure of designed MG-2, a periodic metallic slit array (gray region) filled with two different kinds of media (colored blue regions) alternatively, forming a supercell containing two unit cells (i.e., $m = 2$). (b) Iso-frequency diagram indicating all possible diffraction orders. (c) is the magnetic field patterns for normally incident light.

beam that is normally incident onto it and passes through it into two parts, with their refraction angle of $\theta_t = \pm 45°$.

3. Results and Discussions

Next, we consider the case of bi-layer MGs by simply putting two single-layer MGs together (see Fig. 3). By suitably adjusting the air gap, asymmetric transmission could be obtained. In particular, for PI, most incident light is reflected due to the feature of MG-1 [see Fig. 3(a)], while for NI, beam splitting with high efficiency occurs when the incident wave passes through MG-2 and then through MG-1 [see Fig. 3(b)]. Figure 4(a) presents the numerically calculated relationship between the transmission/reflection and the gap size Δ for both PI and NI. It is clearly seen that for PI, the increasing Δ leads to the transmission efficiency (the dashed black curve) that gradually decreases and goes to zero. For NI, as the Δ increases, the transmission (the dashed blue curve) oscillates with it, due to the multiple scattering of light inside the air gap, and the efficiency always maintains a high transmittance (> 90%). In particular, at $\Delta = 0.25\lambda$ (indicated by the red dashed line), the transmission efficiency for PI and NI is 2% and 92.5%, respectively.

Numerical simulations using Gaussian beams were carried out to demonstrate the performance of asymmetric transmission in bi-layer MGs. For comparison, two cases of $\Delta = 0$ and $\Delta = 0.25\lambda$ are discussed separately. For the case of $\Delta = 0$, Figs. 4(b) and 4(c) show the field patterns for PI and NI, respectively. Clearly, for the incident light with a wavelength $\lambda = 650$ nm, the beam splitting is well demonstrated whether it is PI or NI, in spite of a little bit reflection. For the case of $\Delta = 0.25\lambda$, as shown in Fig. 4(d), the PI beam is almost totally reflected by MG-1. The extremely low transmitted light stems from the evanescent wave bounded at the outgoing interface of MG-1 that tunnels through MG-2, leading to weak beam splitting. By contrast, the field pattern in Fig. 4(e) displays that the NI beam is firstly split in the air gap and then propagates through MG-1. As a result, the

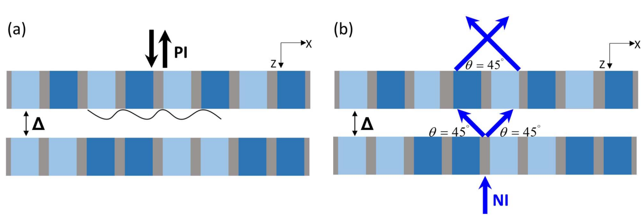

Fig. 3. Structure of designed bi-layer MG system based on MG-1 and MG-2. (a) and (b) schematically show the scattering process for (a) positive incidence (PI) and (b) negative incidence (NI), respectively.

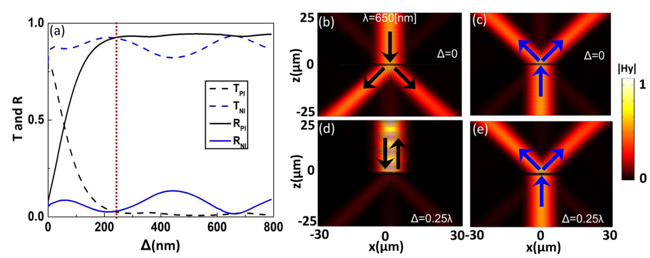

Fig. 4. (a) When the TM wave is incident to the bi-layer MGs, which are filled with impedance-matched material, the relationship curve between the transmission and reflection efficiency and the size of the air gap for PI and NI, respectively. Magnetic field diagram when the air gap with $\Delta = 0$ for (b) PI and (c) NI, and magnetic field diagram when the air gap with $\Delta = 0.25\lambda$ for (d) PI and (e) NI.

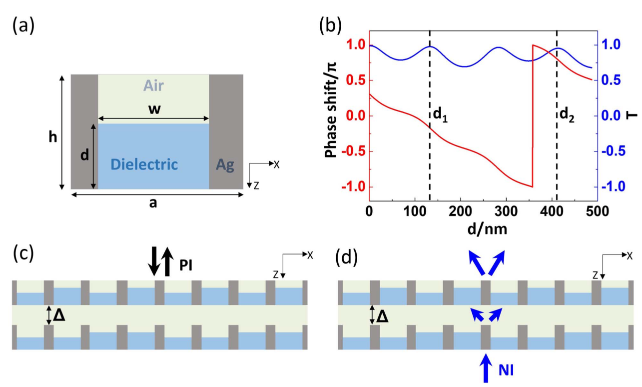

Fig. 5. (a) Geometric structure of nonmagnetic unit cell for the design of magnetic MGs based on the local Fabry–Perot (FP) resonances. (b) Transmission and phase shift of the unit cell versus the height d of filled dielectric with $\varepsilon_d = 4$ and $\mu_d = 1$. (c) and (d) show the schematic diagram of the redesigned bi-layer MGs for (c) PI and (d) NI, respectively.

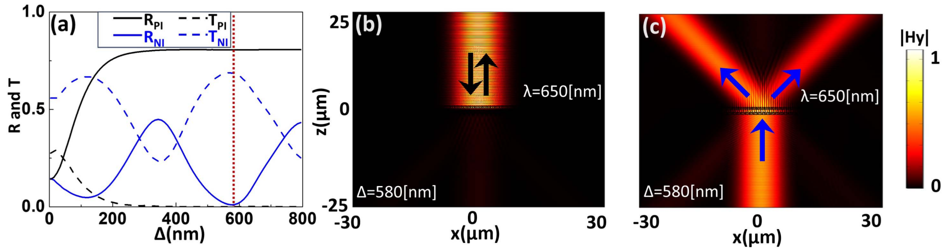

Fig. 6. Performance demonstrations. (a) Relationship between the transmission/reflection efficiency and the size of the air gap for PI and NI. (b) Magnetic field pattern for PI when $\Delta = 580$ nm. (c) Magnetic field pattern for NI when $\Delta = 580$ nm.

transmitted waves are two outgoing beams as expected. Therefore, high-efficiency asymmetric transmission is achieved by adjusting the size of the air gap of the bi-layer MGs composed of MG-1 and MG-2.

Although the impedance-matched material is used in the above discussions, similar results can be obtained by using nonmagnetic dielectrics. To demonstrate this point, here we employ the concept of local Fabry–Perot (FP) resonances[31] in metasurfaces to redesign the single-layer MG. Figure 5(a) shows its new unit cell, a silver slit array filled with a nonmagnetic dielectric of $\varepsilon_d = 4$ and $\mu_d = 1$ (the blue area). The light green area represents the air. Here, $h = 0.75\lambda$ and $w = 180$ nm. For incident light with $\lambda = 650$ nm, Fig. 5(b) shows the calculated transmission and phase of light through the designed unit cell, in which a series of local FP resonances with $T = 1$ can be seen. In particular, when $d_1 = 133$ nm and $d_2 = 406.5$ nm, as indicated by the black dashed line in Fig. 5(b), their phase shift is π, which fully meets the requirements of PGM with two unit cells ($m = 2$). Figures 5(c) and 5(d) show the corresponding geometric diagram of the bi-layer structure designed using such nonmagnetic MGs for the realization of asymmetric transmission.

Such a designed bi-layer MG exhibits good performance. Figure 6(a) presents the numerically calculated relationship between the transmission/reflection and the gap size for both PI and NI. Likewise, as Δ increases from zero, for PI, the transmission gradually decreases and goes to zero. Unlike the impedance-matched case, the saturated reflection efficiency reduces to 80%, due to the more absorption. For NI, as shown by the blue curve in Fig. 6(a), similar oscillation is seen in the transmission spetrum. In particular, when $\Delta = 580$ nm [see the red dotted line in Fig. 6(a)], for NI, the transmission is $T = 1\%$. For PI, the efficiency of optical beam splitting is $T = 69\%$. Such an efficiency is much higher than that previously reported in dielectric PGMs[29], where the splitting efficiency is below 50%. The metals are often considered to be with higher loss at visible wavelengths than the dielectric. Our results show that the metallic PGMs can also exhibit a better perfomance than dielectric-based ones, because of stronger layer interaction enabled by surface plasmons. Moreover, Figs. 6(b) and 6(c) illustrate the corresponding simulated field patterns when a Gaussian beam with the wavelength of $\lambda = 650$ nm is incident on the bi-layer MGs from PI and NI, respectively. The calculated results confirm our findings. Therefore, the effect of asymmetric transmission could still be achieved when the bi-layer MGs are filled with impedance-mismatched materials.

4. Conclusion

In summary, we have designed and studied a bi-layer MG at the visible frequencies, with each MG consisting of subwavelength metal slit arrays with phase-gradient modulation. Based on the found reversed diffraction law, we have shown that the interlayer interaction can produce a transition from optical beam splitting to high-efficiency asymmetric transmission of incident light from two opposite directions. Numerical simulations fully confirm our findings. Due to the tolerance[21,24] in designing the metasurface with discrete unit structures, such a bi-layer MG has a certain broadband response. We have numerically proved that the asymmetric transmission remains good for working wavelengths from 600 nm to 700 nm, although it is designed at the target wavelength of 650 nm. The effect of efficient asymmetric transmission provides unlimited possibilities for potential applications, such as optical multi-functional devices[32], optical imaging systems[33], and optical communication systems[34].

Acknowledgement

This work was supported by the National Natural Science Foundation of China (Nos. 11974010, 11904169, 61705200, 11604229, and 11774252), the Natural Science Foundation of Jiangsu Province (Nos. BK20171206 and BK20190383), the China Postdoctoral Science Foundation (No. 2018T110540), and the Priority Academic Program Development (PAPD) of Jiangsu Higher Education Institutions.

References

1. A. V. Kildishev, A. Boltasseva, and V. M. Shalaev, “Planar photonics with metasurfaces,” Science **339**, 1232009 (2013).
2. N. M. Estakhri and A. Alù, “Recent progress in gradient metasurfaces,” J. Opt. Soc. Am. B **33**, A21 (2016).
3. Y. Xu, Y. Y. Fu, and H. Chen, “Planar gradient metamaterials,” Nat. Rev. Mater. **1**, 16067 (2016).
4. S. Sun, Q. He, and L. Zhou, “Electromagnetic metasurfaces: physics and applications,” Adv. Opt. Photon. **380**, 479 (2016).

5. N. Yu, P. Genevet, M. A. Kats, F. Aieta, J.-P. Tetienne, F. Capasso, and Z. Gaburro, "Light propagation with phase discontinuities: generalized laws of reflection and refraction," Science **334**, 333 (2011).
6. S. Wang, P. C. Wu, V.-C. Su, Y.-C. Lai, M.-K. Chen, H. Y. Kuo, B. H. Chen, Y. H. Chen, T.-T. Huang, J.-H. Wang, R.-M. Lin, C.-H. Kuan, T. Li, Z. Wang, S. Zhu, and D. P. Tsai, "A broadband achromatic metalens in the visible," Nat. Nanotech. **13**, 227 (2018).
7. P. Genevet, J. Lin, M. A. Kats, and F. Capasso, "Holographic detection of the orbital angular momentum of light with plasmonic photodiodes," Nat. Commun. **3**, 1278 (2012).
8. X. Yin, Z. Ye, J. Rho, Y. Wang, and X. Zhang, "Photonic spin Hall effect at metasurfaces," Science **339**, 1405 (2013).
9. T. J. Cui, M. Q. Qi, X. Wan, J. Zhao, and Q. Cheng, "Coding metamaterials, digital metamaterials and programmable metamaterials," Light: Sci. Appl. **3**, e218 (2014).
10. X. Ni, Z. J. Wong, M. Mrejen, Y. Wang, and X. Zhang, "An ultrathin invisibility skin cloak for visible light," Science **349**, 1310 (2015).
11. A. M. H. Wong and G. V. Eleftheriades, "Perfect anomalous reflection with a bipartite Huygens' metasurface," Phys. Rev. X **8**, 011036 (2018).
12. J. Yan, Y. Guo, M. Pu, X. Li, X. Ma, and X. Luo, "High-efficiency multi-wavelength metasurface with complete independent phase control," Chin. Opt. Lett. **17**, 050003 (2018).
13. L. Li, Q. Yuan, R. Chen, X. Zou, W. Zang, T. Li, G. Zheng, S. Wang, Z. Wang, and S. Zhu, "Chromatic dispersion manipulation based on metasurface devices in the mid-infrared region," Chin. Opt. Lett. **18**, 082401 (2020).
14. L. Zhang, J. Ding, H. Zheng, S. An, H. Lin, B. Zheng, Q. Du, G. Yin, J. Michon, Y. Zhang, Z. Fang, M. Y. Shalaginov, L. Deng, T. Gu, H. Zhang, and J. Hu, "Ultra-thin high-efficiency mid-infrared transmissive Huygens meta-optics," Nat. Commun. **9**, 1481 (2018).
15. Y. Ra'di, D. L. Sounas, and A. Alù, "Metagratings: beyond the limits of graded metasurfaces for wave front control," Phys. Rev. Lett. **119**, 067404 (2017).
16. N. Estakhri, V. Neder, M. Knight, A. Polman, and A. Alù, "Visible light, wide-angle graded metasurface for back reflection," ACS Photon. **4**, 228 (2017).
17. H. Wang, J. Zheng, Y. Fu, C. Wang, X. Huang, Z. Ye, and L. Qian, "Multichannel high extinction ratio polarized beam splitters based on metasurfaces," Chin. Opt. Lett. **17**, 052303 (2019).
18. Y. Xu, Y. Fu, and H. Chen, "Steering light by a sub-wavelength metallic grating from transformation optics," Sci. Rep. **5**, 12219 (2015).
19. E. Qian, Y. Fu, Y. Xu, and H. Chen, "Total omnidirectional reflection by sub-wavelength gradient metallic gratings," Europhys. Lett. **114**, 34003 (2016).
20. Y. Fu, Y. Cao, and Y. Xu, "Multifunctional reflection in acoustic metagratings with simplified design," Appl. Phys. Lett. **114**, 053502 (2019).
21. Y. Fu, C. Shen, Y. Cao, L. Gao, H. Chen, C. T. Chan, S. A. Cummer, and Y. Xu, "Reversal of transmission and reflection based on acoustic metagratings with integer parity design," Nat. Commun. **10**, 2326 (2019).
22. Y. Li, C. Shen, Y. Xie, J. Li, W. Wang, S. A. Cummer, and Y. Jing, "Tunable asymmetric transmission via lossy acoustic metasurfaces," Phys. Rev. Lett. **119**, 035501 (2017).
23. X. Wang, A. Díaz-Rubio, V. S. Asadchy, G. Ptitcyn, A. A. Generalov, J. Ala-Laurinaho, and S. A. Tretyakov, "Extreme asymmetry in metasurfaces via evanescent fields engineering: angular-asymmetric absorption," Phys. Rev. Lett. **121**, 256802 (2018).
24. Y. Cao, Y. Fu, Q. Zhou, X. Ou, L. Gao, H. Chen, and Y. Xu, "Mechanism behind angularly asymmetric diffraction in phase-gradient metasurfaces," Phys. Rev. Appl. **12**, 024006 (2019).
25. Y. Fu, J. Tao, A. Song, Y. Liu, and Y. Xu, "Controllably asymmetric beam splitting via gap-induced diffraction channel transition in dual-layer binary metagratings," Front. Phys. **15**, 52502 (2020).
26. G. Hu, A. Krasnok, Y. Mazor, C. Qiu, and A. Alù, "Moiré hyperbolic metasurfaces," Nano. Lett. **3217**, 3224 (2020).
27. G. Hu, Q. Ou, G. Si, Y. Wu, J. Wu, Z. Dai, A. Krasnok, Y. Mazor, Q. Zhang, Q. Bao, C. Qiu, and A. Alù, "Observation of topological polaritons and photonic magic angles in twisted van der Waals bi-layers," Nature **582**, 209 (2020).
28. S. Chen, Y. Zhang, Z. Li, H. Cheng, and J. Tian, "Empowered layer effects and prominent properties in few-layer metasurfaces," Adv. Opt. Mater. **22**, 181477 (2020).
29. D. Zhang, M. Ren, W. Wu, N. Gao, X. Yu, W. Cai, X. Zhang, and J. Xu, "Nanoscale beam splitters based on gradient metasurfaces," Opt. Lett. **43**, 267 (2018).
30. H. Shi, C. Wang, C. Du, X. Luo, X. Dong, and H. Gao, "Beam manipulating by metallic nano-slits with variant widths," Opt. Express **13**, 6815 (2005).
31. Y. Cao, B. Yu, Y. Fu, L. Gao, and Y. Xu, "Phase-gradient metasurfaces based on local Fabry–Pérot resonances," Chin. Phys. Lett. **37**, 097801 (2020).
32. S. Zhu, Y. Cao, Y. Fu, X. Li, L. Gao, H. Chen, and Y. Xu, "Switchable bifunctional metasurfaces: nearly perfect retroreflection and absorption at the terahertz regime," Opt. Lett. **45**, 3992 (2020).
33. B. Yao, X. Zang, Z. Li, L. Chen, J. Xie, Y. Zhu, and S. Zhuang, "Dual-layered metasurfaces for asymmetric focusing," Photon. Res. **8**, 830 (2020).
34. A. Yi, L. Yan, Y. Pan, L. Jiang, Z. Chen, W. Pan, and B. Luo, "Transmission of multi-dimensional signals for next generation optical communication systems," Opt. Commun. **408**, 42 (2017).